Sub-meV photoluminescence linewidth and >10^6 cm^2/Vs electron mobility in AlGaAs/GaAs quantum wells grown by metalorganic vapor phase epitaxy on slightly misoriented substrates

E. Pelucchi, N. Moret, B. Dwir, D. Y. Oberli, A. Rudra, N. Gogneau, A. Kumar, and E. Kapon
Ecole Polytechnique Fédérale de Lausanne (EPFL), Laboratory of Physics of Nanostructures, CH-1015 Lausanne, Switzerland

E. Levy and A. Palevski
School of Physics and Astronomy, Tel-Aviv University, Tel Aviv, Israel

(Received 13 February 2006; accepted 12 March 2006; published online 15 May 2006)

We report sub-meV (as low as 0.6 meV) low-temperature photoluminescence linewidth and high low-temperature electron mobility ($\mu \sim 1-1.5\times10^6$ cm^2/Vs) of GaAs quantum wells in AlGaAs barriers grown by standard metalorganic vapor phase epitaxy. These records values are achieved by epitaxial growth on (100) slightly misoriented substrates [$\leqslant$0.6 degrees off-(100) GaAs substrates] in combination with a high V/III ratio for AlGaAs growth. Such small misorientations are sufficient to drastically modify the optical and transport properties as well as the growth mode and surface morphologies of both GaAs and AlGaAs epitaxial layers, allowing greater interface quality and reduced impurity incorporation. The quantum wells so obtained show optical properties comparable to high-quality samples grown by molecular beam epitaxy. In addition, the slight misorientation considerably reduces the impact of substrate temperature on electron mobility, which allows achieving high values of μ within a much broader range of growth temperatures. © *2006 American Institute of Physics*. [DOI: 10.1063/1.2195370]

I. INTRODUCTION

The properties of III-V semiconductor quantum wells (QWs) have been the subject of intense research effort, motivated by their use in fundamental studies in solid state physics for both optical[1–4] and transport studies,[5,6] as well as in important applications in electronic and optoelectronic devices. On the applications front, III-V QWs are at the very heart of many everyday-use and industrial semiconductor lasers, while high-electron-mobility transistors based on III-V compound semiconductor heterostructures have become the main electronic component in a wide range of systems including mobile telephones, radio telescopes, satellite television receivers and satellite navigation devices.[7] These components rely on both high-quality epitaxial layers as well as on cost-effective, large-scale production facilities. In this context, metalorganic vapor phase epitaxy (MOVPE) is often the crystal growth technique of choice.

The key ingredients for obtaining high-quality III-V heterostructures are low impurity incorporation and well-controlled interfaces. Useful parameters for assessing the combined purity and interface quality of QW structures is their low-temperature photoluminescence (PL) linewidth and the electron mobility in modulation doped structures.[8] Concerning the optical properties, several groups have reported sub-meV low-temperature PL linewidths for GaAs/AlGaAs QWs grown by molecular beam epitaxy (MBE).[2,9] Moreover, the perpetual quest for higher electron mobilities, pursued mainly with compound semiconductors grown by MBE, has led to record values as high as $\mu=3.1\times10^7$ cm^2/Vs for 30 nm thick GaAs/AlGaAs quantum wells (QWs) at low temperatures.[6] Such narrow linewidths and high mobility materials are particularly important for investigating the fine structure of confined excitons and exciton complexes[1,2,4] or novel electrical transport phenomena such as the fractional quantum Hall effect.[5]

Metalorganic vapor phase epitaxy has not reached so far this level of quality. On the optics side, low-temperature PL spectra of ~9–10 nm GaAs/AlGaAs QWs showing full width at half maximum (FWHM) of ~4.0/~2.5 meV, reported by Dupuis *et al.*[10] and Kuech *et al.*,[11] respectively, represent some of the best results published so far by other groups.[12] Actually, no major improvement in the optical properties of GaAs in AlGaAs QWs by MOVPE appears to have been reported in the last 20 years.[13] Moreover, if compared to MBE, MOVPE-grown materials have traditionally shown lower electron-mobility values and significant reproducibility difficulties, normally attributed to both reactor and precursor purity issues. The highest mobility by MOVPE to date was demonstrated by Chui *et al.*,[14] who have measured $\mu=2\times10^6$ cm^2/Vs in a GaAs/AlGaAs (single interface) heterojunction under illumination at 0.3 K, with a two-dimensional electron gas (2DEG) carrier density of $n=3.2\times10^{11}$ cm^{-2} and using tertiarybutylarsine as group V precursor. The highest mobility reported with the conventional group V precursor arsine is 1.3×10^6 cm^2/Vs with a carrier density of $n=4.8\times10^{11}$ cm^{-2}.[15] All these results were obtained with AlGaAs/GaAs heterojunctions, which expose the 2DEG to a single AlGaAs interface and thus should be less sensitive to interface roughness and scattering from charged impurities in the AlGaAs layers as compared to QW double heterostructures. To the authors' knowledge, no sig-

nificantly high mobilities have been reported for GaAs QWs grown by MOVPE with AlGaAs barriers, irrespective of the group V precursor choice.

It should be emphasized, however, that the growth mechanisms involved in MOVPE are very different and more complex than those underlying MBE, particularly as they include precursor molecule transport and decomposition. Hence, more insight into the parameters affecting the crystalline and electronic quality of semiconductor QWs grown by MOVPE is much needed. In this context, the effect of substrate misorientation on the PL spectra of GaAs/AlGaAs QWs grown by MOVPE has been already investigated. Several publications report the analysis of the surface morphologies of the annealed GaAs surface layers in an attempt to correlate them with the PL properties of the active QW layers. Substrate misorientation with respect to the (100) planes has been shown to give rise to different surface ordering and/or step arrangements. While earlier studies[16,17] had covered misorientations in the 0.5°–8° range (in fact, irrespectively of the growth technique used), we recently reported[12] that even smaller offsets (0.2–0.3 degrees) from the nominal (100) surface significantly affect the optical properties of GaAs/AlGaAs QWs. Significant electron mobility values, about 5×10^5 cm^2/Vs, were also reported for MOVPE-grown 2DEG GaAs/AlGaAs QW structures made on 0°–0.3° misoriented (100) substrates with a nonoptimized sample structure.[12] However, the mechanisms and limits of this approach concerning electrical transport have not yet been addressed.

In this work we report on an investigation of the remarkable effects of small substrate misorientations (and surface morphology) on both the optical properties and the electron mobilities of GaAs/AlGaAs QWs and 2DEG structures grown by MOVPE using AsH_3 as a group V precursor. We obtained a substantial improvement for the low-temperature PL linewidths and for the electron mobilities by further optimization and extended range of growth parameters. Record photoluminescence full widths at half maximum, as low as 0.6 meV for 15 nm thick GaAs/$Al_{0.3}Ga_{0.7}As$ QWs, were observed. Record low-temperature (1.4 K) electron mobilities, as high as ~1.5 million cm^2/Vs, in a 14 nm thick QW with a two-dimensional (2D) carrier density of 4.6×10^{11} cm^{-2} without illumination, were also achieved. We show here that two main ingredients are necessary for attaining such values: a proper choice of substrate vicinal surface in the range 0.1°–0.6° off the perfect (100) orientation, and a specific combination of growth conditions, particularly V/III ratio, growth temperature, and growth rate.

II. EXPERIMENTAL DETAILS

The samples were grown in a commercial, horizontal MOVPE reactor at 20 mbar using trimethylgallium, trimethylaluminum and purified arsine. Disilane was used as the *n*-type dopant source, while purified nitrogen was used as a carrier gas. Two sets of samples were grown, one dedicated to photoluminescence studies, the other to transport characterization. It is important to observe that the two sets of sample do not perfectly overlap in terms of "best" growth parameters as a result of our optimization procedure. Nevertheless, for all the samples, the growth rate was kept at 1 μ/h (~1 monolayer/s) for the $Al_yGa_{1-y}As$ layers. Growth temperatures (we will refer here always to the estimated surface temperature) and (100) substrate misorientation [always off-(100) towards the [111]*A* direction ±0.02°] were varied as described in the text.

The samples for the optical studies included 3 GaAs quantum wells (2, 5, and 15 nm thick) separated by 300 nm thick $Al_{0.3}Ga_{0.7}As$ barriers, with a 30 nm thick GaAs cap. The buffer consisted of 500 nm GaAs and 500 nm $Al_{0.3}Ga_{0.7}As$ layers. The quoted layer thicknesses and concentrations are the nominal values. The V/III ratio was different for the GaAs layers and for the $Al_{0.3}Ga_{0.7}As$ as stated in the text. No growth interruption was performed. Photoluminescence (PL) spectra were acquired at 10 K (unless otherwise stated) with the samples mounted on the cold finger of a helium-flow cryostat and excited using the 514 nm line of an Ar-ion laser.

All transport structures were identical with the exception of the growth temperature (T_g) and for the substrate choice, with misorientations varying from "exactly" (100) to 0.6° off. They consisted of 300 nm GaAs buffer, 500 nm $Al_{0.27}Ga_{0.73}As$ buffer, 30 nm Si-doped ($\sim2\times10^{18}$ cm^{-3}) $Al_{0.27}Ga_{0.73}As$ layer, 80 nm undoped $Al_{0.27}Ga_{0.73}As$ spacer, 14 nm GaAs QW, 30 nm undoped $Al_{0.27}Ga_{0.73}As$ spacer, 30 nm Si-doped $Al_{0.27}Ga_{0.73}As$ layer, 100 nm undoped $Al_{0.27}Ga_{0.73}As$ spacer, and 10 nm undoped GaAs cap layer. The V/III ratio was 100 for the GaAs layers and 300 for the $Al_{0.27}Ga_{0.73}As$. The electron mobility of the samples was evaluated by standard Hall bars using four-contact ac (lock-in) measurement at a current of 1 μA at 4.2 K.

The GaAs cap morphology was probed by atomic force microscopy (AFM) in noncontact mode. Reference samples consisting of 230 nm $Al_{0.27}Ga_{0.73}As$ layers were grown under the same conditions of the transport samples for studying the AlGaAs morphology as well using AFM.[18]

In all cases, particular attention was paid to reactor environment quality and to temperature control, by growing the samples only with reactor walls already baked and covered by previous growths.[19]

III. PHOTOLUMINESCENCE VERSUS SUBSTRATE MISORIENTATION

To investigate the impact of the substrate misorientation on the QW optical properties, we systematically studied the PL spectra as a function of the substrate miscut. For this part of the study, the V/III ratio was chosen to be 220 or 280 for the $Al_{0.3}Ga_{0.7}As$ layers and 130 for GaAs QW, and the growth temperature was fixed at ~690 °C, if not otherwise stated. A representative spectrum, showing the PL emitted by the three QWs and the AlGaAs layers, is presented in the inset of Fig. 1(a). The main part of Fig. 1(a) shows the PL line full width at half maximum (FWHM) as a function of substrate misorientation[20] for the three QWs, in the misorientation range 0°–0.6° off.

The general trend is immediately evident. A perfectly (100) oriented substrate yields significantly broader line-

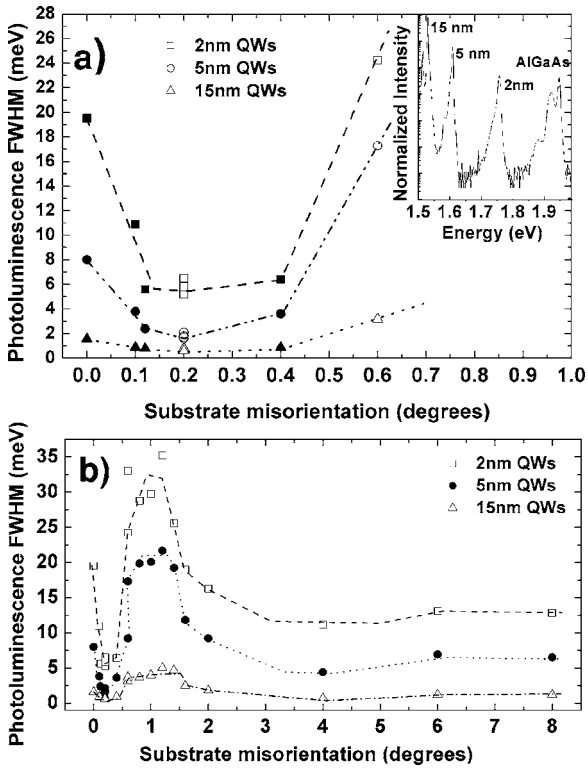

FIG. 1. (a) (Inset) Representative low-temperature PL spectrum of a GaAs/AlGaAs QW sample showing spectral lines corresponding to the three wells (2, 5, 15 nm) and the $Al_{0.30}Ga_{0.70}As$ barriers. (Main) QW photoluminescence FWHM as a function of substrate misorientation toward (111)*A* for three different QW thicknesses. Experimental points with filled symbols were obtained in the same epitaxial run, whereas the others had identical nominal growth conditions (see text). Dashed and dotted lines are guides to the eye; (b) QW PL FWHM as a function of substrate misorientation toward (111)*A* for the same three different QW thicknesses in a broader misorientation range. The data correspond to different growth runs with identical growth conditions as in (a). All growths were performed also on a 0.2° off control sample to guarantee that the FWHM measured are not artifacts. Dashed and dotted lines are guides to the eye.

widths as compared with small misorientations, especially for the thinner QWs, while at 0.6° off-(100), a significant increase in the PL spectrum linewidth can again be observed. The 2, 5, and 15 nm QW samples show FWHM values that decrease, respectively, from ~20, 8, and 1.6 meV to 5.2, 1.6, and 0.60 meV in our best samples grown on 0.2° misoriented substrates.[21] It is noteworthy that the FWHM values for our 15 nm QWs are all well below values previously reported in the literature, even for the perfectly oriented samples. In general, all our samples grown on misoriented substrates in the misorientation interval 0.12–0.4 degrees show significantly narrower PL linewidths than other reported values for comparable QW thicknesses[10] (which usually are well above 6–8 meV for thin QWs); e.g., the QW FWHMs of the 2 and 5 nm range between 6.4 meV and 5.2 meV, and 3.6 and 1.6 meV, respectively.

On the other hand, as shown in Fig. 1(b), where we present data more broadly spaced in the 0°–8° off range, the FWHMs show a broad maximum for all three QW thicknesses around 1° off-(100), while at higher misorientations the FWHMs decrease again, without generally reaching the best values obtained in the small misorientation range. It is worth noticing that the FWHM for the thinnest QW around

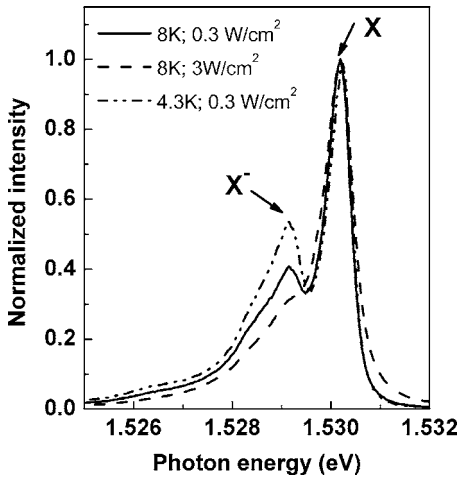

FIG. 2. PL spectrum of the best 15 nm QW sample at different pumping levels and temperature. The main low-energy shoulder is assigned to the negatively charged trion.

1° off-(100) shows a maximum around 30–35 meV, i.e., some seven times higher than the samples grown on 0.2° off substrates. It is also noticeable that the 15 nm QW grown at 4° off-(100) presents a FWHM of 0.7 meV. This value is within the best we observed. However, in the same sample the QWs of 5 nm and 2 nm showed a FWHM of 4.4 and 11.2 meV, well above the values observed in the small misorientation range.

In Fig. 2 we show the PL spectrum of the 15 nm QW line in one of our best QW sample, grown with a V/III ratio of 220 for AlGaAs and 130 for GaAs on a 0.2° misoriented substrate. The spectrum features a low linewidth of 0.6 meV for the 15 nm QW. The photoluminescence was excited with Ar-ion laser at a power density of 300 mW/cm^2 and a temperature of 4.3 K. The linewidth increased to 0.67 meV at a temperature of 8 K and a power density of 3 W/cm^2. By lowering either the power density or the temperature, a new line appeared on the low-energy side of the main exciton transition. This peak is assigned to the negatively charged trion based on its binding energy of 1.1 meV (Refs. 1 and 2) and on the temperature dependence of the peak intensity. Shoulders on the low-energy side of this emission line originate from excitons bound to neutral donors probably due to unintentional background doping of the GaAs layer.

Several other samples were grown in order to investigate the reproducibility and repeatability of the PL spectra as well as the dependence on several growth parameters around the optimal conditions we determined. We found that the optimal growth temperature range is centered at ~690 °C, with a significant PL emission line broadening at lower temperatures (FWHM at 660 °C for the 15, 5, and 2 nm QWs of 1.6, 8.2, and 10 meV, respectively, on a 0.2° misoriented substrate), whereas a minor broadening was observed at 720 °C. A V/III ratio for the AlGaAs layers of 220 and 280 was used without significant variations of the QW PL linewidth (FWHM for the 15 nm QWs always ranging between 0.7 and 0.8 meV), whereas a strong increase in the FWHM was observed for ratios below 180. Conversely, only a very moderate broadening could be measured when the V/III ratio was raised to 320.

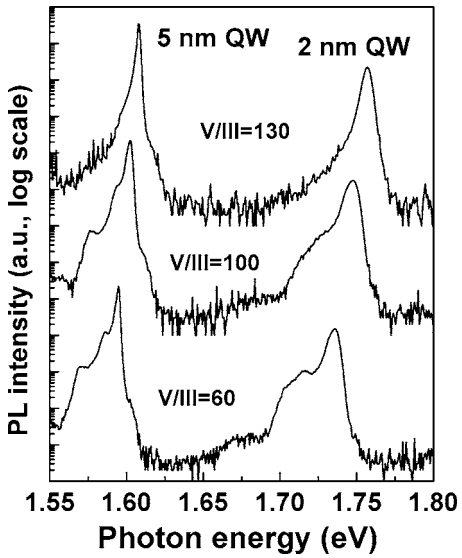

FIG. 3. Spectrum evolution as a function of the V/III ratio (60, 100, 130) for GaAs at fixed V/III ratio=280 for AlGaAs, for the 5 and the 2 nm QWs. Growth temperature was ~690 °C for all samples.

To further illustrate the effect of the V/III ratio on the PL spectra, we show in Fig. 3 the spectrum evolution as a function of this ratio for GaAs growth (60, 100, 130) at a fixed AlGaAs V/III ratio of 280, for QW thicknesses of 5 and 2 nm. Growth temperature was ~690 °C and the substrate was misoriented by 0.2°. All other growth parameters were nominally identical. The main excitonic peaks show moderate differences in the three samples (for example, the 5 nm QW shows a FWHM of 3.1 meV for a V/III=100, which reduces to 1.6 meV for a V/III=130) and can be substantially compared, for both QWs, to those found in our previous samples. On the other hand, using a high V/III ratio for the GaAs QW growth significantly reduces the intensity of the low-energy shoulders of the excitonic peaks. These shoulders, which originate from excitons bound on impurities, from donor acceptor pair recombination and free to bound carrier recombination, are extremely pronounced in the sample with a V/III ratio of 60 but disappear for a V/III ratio of 130. This demonstrates a significant sensitivity of impurity incorporation in the QW layer on the As flux. A similar but less pronounced trend was also found for the 15 nm QW (not shown).

We finally observe that, as a general trend, samples having larger FWHM also usually showed a slightly redshifted peak emission when compared to the best FWHM samples. A more detailed analysis of this effect will be presented elsewhere.[22]

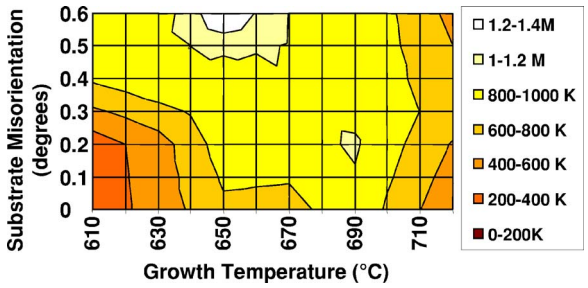

FIG. 4. (Color online) Pictorial representation of the data in Table I using contour plots in the substrate misorientation-growth temperature plane. The missing data in the rectangular mesh where linearly interpolated.

IV. TRANSPORT PROPERTIES VERSUS SUBSTRATE MISORIENTATION

We observed a similar strong dependence of the transport properties on small substrate misorientations. Table I summarizes the electron mobilities measured for different substrate orientations and (estimated) growth temperatures. We measured the mobility of all samples along both the [01-1] and [011] directions; however, no systematic differences could be found between the two crystalline orientations. Samples appearing in the same temperature column in Table I were grown in the same growth run, with the exception of T_g=650 °C, for which the experimental data are extracted from two independent growth runs. In a quest for trends in the values of the mobility, the data of Table I are presented in Fig. 4 by means of contour plots in the temperature-misorientation plane.

The highest mobility, $\sim 1.39\times10^6$ cm^2/Vs (1.48×10^6 cm^2/Vs) measured at 4.2 K (1.4 K) was obtained at a substrate misorientation of 0.6 degrees and at growth temperature of 650 °C. The point of highest mobility in Fig. 4 is surrounded by a broad region of mobilities close to or above 0.8×10^6 cm^2/Vs, with further decrease occurring at the borders of the considered parameter space. Moreover, we observe that a substrate misorientation of 0.6 degrees is very tolerant to variations in growth temperature, showing high mobility in all but the very high-temperature range (720 °C).

On the contrary, when a perfectly oriented substrate was chosen, a strong dependence of the mobility on growth temperature was obtained. The mobility showed a relatively poor

TABLE I. Sample mobilities as a function of substrate misorientation and growth temperature as measured at 4.2 K. The GaAs surface type classification, given in parentheses, are discussed in the text.

Substrate misorientation (degrees)	Mobility at T_g=610 °C (10^3 cm^2/Vs)	Mobility at T_g=630 °C (10^3 cm^2/Vs)	Mobility at T_g=650 °C (10^3 cm^2/Vs)	Mobility at T_g=670 °C (10^3 cm^2/Vs)	Mobility at T_g=690 °C (10^3 cm^2/Vs)	Mobility at T_g=720 °C (10^3 cm^2/Vs)
0	270 (II)	485 (II)	784 (II)	723 (II)	946 (I)	437 (I)
0.2	291 (III)	507 (III)	900 (III)	914 (III)	1020 (V)	584 (V)
0.3	-	-	894 (III)	972 (V)	956 (V)	718 (VI)
0.4	833 (III)	967 (III)	797 (IV)	-	-	-
0.6	907 (IV)	866 (IV)	1390 (V)	992 (V)	989 (VI)	541 (VI)

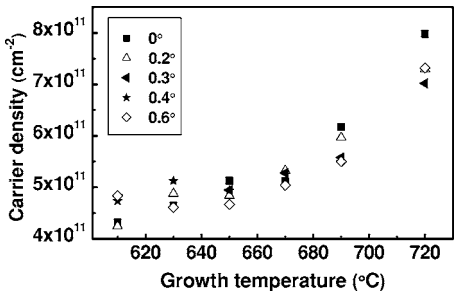

FIG. 5. Two-dimensional carrier density measured for the samples of Table I as a function of substrate misorientation at different growth temperatures.

value of 270×10^3 cm^2/Vs at low-growth temperatures, which is 3.5 times lower than the best value obtained on a nearly exact substrate (946×10^3 cm^2/Vs) and nearly five times lower than the best value obtained for 0.6° off-(100) substrates. Only at relatively high temperatures (690 °C) do mobilities reach values comparable to those obtained with substrates with higher misorientations. A similar trend with growth temperature is exhibited by the growth on 0.2° off-(100) substrates, yielding relatively poor mobilities at 610 °C and 630 °C. High mobilities at low-growth temperatures are obtained only above ~0.4° misorientations.

The measured 2D carrier density versus the growth temperature is shown in Fig. 5 for the different substrate misorientations. The carrier density increases with growth temperature, particularly above 660 °C, but no significant trend with increasing substrate misorientation is observed. The rather sharp increase in carrier density above 690 °C is correlated with the general deterioration in mobility for all misorientations used. This is probably due to an increase in the background doping level in the barriers at this temperature.

V. SURFACE MORPHOLOGIES

We observed an extremely broad range of surface morphologies (mostly previously unreported) in the temperature-misorientation plane for both GaAs and AlGaAs layers, even within a narrow range of parameters. Here we limit our analysis to the misorientation range 0°–0.6° off-(100) for both sample sets. A snapshot of the different surfaces observed is presented in Figs. 6 and 7, representative of the optical and transport sample surfaces, respectively.

We assigned a roman ordinal to each surface type [see Figs. 6 and 7; three-dimensional (3D) views, flattened images, and line scans are alternated for better clarity] and reported them in Table I (GaAs only). We indicated as type I [Figs. 6(a) and 7(e)] and type II (not shown) surfaces evidencing a *step flow* and *step flow with islanding* profile, re-

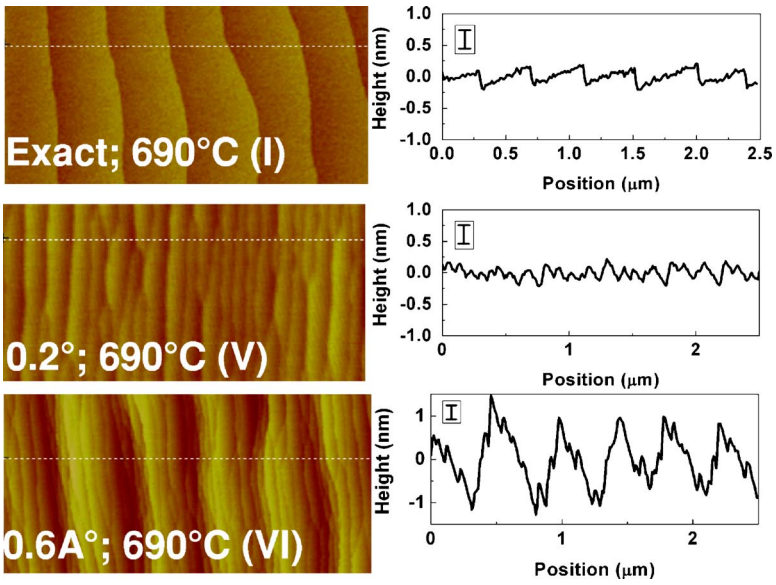

FIG. 6. (Color online) (Left) Noncontact mode representative AFM flattened scans of optical sample GaAs cap surfaces (annealed during sample cooling) for three substrate misorientations of 0°, 0.2°, and 0.6° grown side by side at a temperature of ~690 °C and a V/III ratio of 130 for the GaAs layer. The roman ordinal corresponds to the surface-type classification as discussed in the text. The transition from step flow to step bunching develops in the misorientation range of 0.1° to 0.2° (not shown). (Right) Representative line scans for the three images. The bars in the insets indicate a monolayer step height.

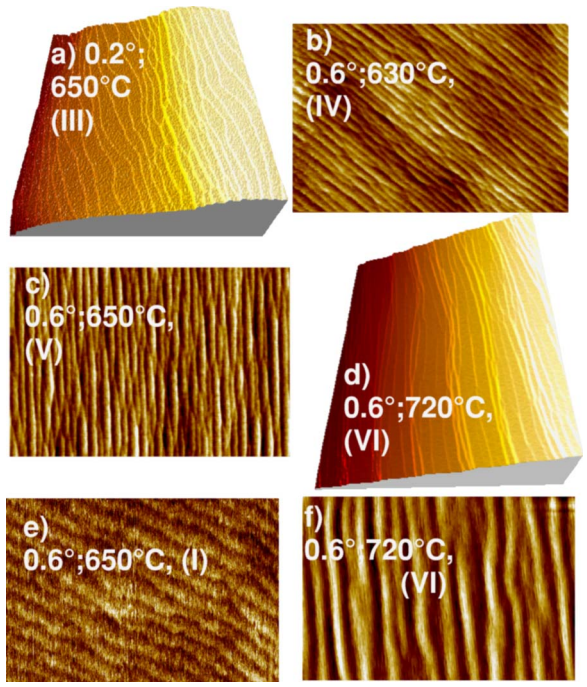

FIG. 7. (Color online) 3D and 2D AFM images of the GaAs cap layer of the 2D electron gas samples (a)–(d) or reference AlGaAs layers (e) and (f) grown on various substrate misorientations and at different growth temperatures as indicated. The roman ordinal corresponds to the surface-type classification as discussed in the text. The step heights range from the 1 monolayer of the step-flow mode to typically 2–4 monolayers in the step-bunched regime. The image sizes are: (a) 3×3 μm; (b) 3×1.5 μm; (c) 3×1.5 μm; (d) 3×3 μm; (e) 0.5×0.25 μm; (f) 5×2.5 μm.

spectively. Type III surfaces [Fig. 7(a)] show an *aperiodic* alternation of step flow and step bunching, while type IV surfaces [Fig. 7(b)] show an *aperiodic* step-bunching profile characterized by different step-bunch heights in different regions. Type V surfaces [Figs. 6(b) and 7(c)] present a *flat step-bunched* GaAs surface (i.e., substantially featureless, with the exception of step branching), and type VI are characterized by a *periodically step-bunched* profile [Figs. 6(c), 7(d), and 7(f)], i.e., a periodic succession of differently step-bunched regions.[23]

It should be mentioned that the onset of the step-bunching regime has been reported to appear for MOVPE growth at misorientations that are strongly dependent on the growth conditions (at variance with MBE grown structures).[24] However, in our case, the two sets of samples do not differ substantially in the V/III ratio parameter choice for a given material, and no major differences could be observed in AFM when identical material, growth temperature, and substrates were chosen.

VI. DISCUSSION

We could not observe an unambiguous correlation between the photoluminescence linewidth, the electron mobility, and surface morphologies. One should expect the morphology details to be linked to a broad range of effects impacting the optical and transport properties: general growth mode and mechanisms,[25] impurity incorporation, and alloy segregation. Nevertheless, we could observe some general trends. The narrower PL linewidths achieved at slight substrate misorientation should be related to a reduced interface disorder and an improved layer-by-layer growth taking place under those conditions. One indication to this effect is the stronger influence of substrate misorientation observed for the thinner QWs. Even though no direct correlation between the embedded QW interface and the upper surface of the annealed structure can be established, as shown recently by Bernatz *et al.*,[26] the differences in surface evolution that we presented should be considered as important markers of the differences in the buried interface structure directly affecting the QW optical properties.[27] In this context, it is noteworthy that the narrowest PL linewidths are obtained for a *flat step-bunched* surface rather than for a *step-flow* pattern of the annealed surface. Moreover, inspection of Table I shows that many (but not all) of our highest mobility structures show a *flat step-bunched* GaAs layer and a *step-flow* AlGaAs pattern, as in the case of our samples with the best optical properties. The lower mobilities, on the other hand, seem to be associated with islanding on perfectly oriented substrates (type II), and, for the smallest misorientations, to a growth mode showing a type III surface for *both* GaAs and AlGaAs. Nevertheless, we should point out that we observed high mobilities ($\sim$1 million cm^2/Vs) also on samples (0.6° misorientation, T_g=690 °C) showing on both GaAs and AlGaAs a periodic step-bunched profile, which in the PL experiments was associated with poor interface quality and optical properties.

In any case, establishing a meaningful correlation between the annealed surface features, the QW interface structure, and the PL and transport characteristics requires further insight into the complex interplay between alloy ordering, impurity incorporation, and impurity screening effects on one hand, and precursors decomposition, adatom diffusion and surface morphology, reconstruction, and chemistry, on the other hand. This might pave the way to further improvements in the optical properties and mobility of such MOVPE-grown structures.

VII. CONCLUSIONS

In conclusion, we demonstrated that by growing on slightly ($<1°$) misoriented (100) GaAs substrates it is possible to obtain a considerable improvement of the optical and transport properties of AlGaAs/GaAs/AlGaAs quantum wells grown by MOVPE using AsH_3 as the group III precursor. Optical properties comparable with high-quality MBE-grown samples were demonstrated, by reproducibly attaining record sub-meV photoluminescence linewidths. Low-temperature electron mobilities $>10^6$ cm^2/Vs were also observed, and, with a proper selection of temperature and substrate orientation, record mobilities in QWs as high as $\sim$1.5 million cm^2/Vs were demonstrated. In particular, the choice of slightly misoriented substrates significantly broadens the growth temperature range for which high mobilities were observed. Such high-optical and transport-quality structures might be useful in studies of optical properties and quantum transport in low-dimensional structures, such as V-groove quantum wire heterostructures[28] relying on the MOVPE growth peculiarities.

ACKNOWLEDGMENTS

We would like to acknowledge the contribution of S. Wüthrich to the photoluminescence data acquisition. The technical assistance of M. Karpovski, V. Shelukhin, I. Sternfeld, and M. Eshkol, is also greatly acknowledged. This work, as part of the European Science Foundation EUROCORES Programme SONS, was supported by funds from the Swiss National Science Foundation and the EC Sixth Framework Programme.

[1] G. Eytan, Y. Yayon, M. Rappaport, H. Shtrikman, and I. Bar-Joseph, Phys. Rev. Lett. **81**, 1666 (1998).
[2] A. Esser, E. Runge, R. Zimmermann, and W. Langbein, Phys. Rev. B **62**, 8232 (2000).
[3] L. V. Butov, A. C. Gossard, and D. S. Chemla, Nature **418**, 751 (2002); D. Snoke, S. Denev, Y. Liu, L. Pfeiffer, and K. West, *ibid.* **418**, 754 (2002).
[4] J. Szczytko, L. Kappei, J. Berney, F. Morier-Genoud, M. T. Portella-Oberli, and B. Deveaud, Phys. Rev. Lett. **93**, 137401 (2004).
[5] J. P. Eisenstein, K. B. Cooper, L. N. Pfeiffer, and K. W. West, Phys. Rev. Lett. **88**, 076801 (2002).
[6] L. Pfeiffer and K. W. West, Physica E (Amsterdam) **20**, 57 (2003).
[7] See, for example: IEEE J. Solid-State Circuits **38**, 1431 (2003).
[8] L. Gottwaldt, K. Pierz, F. J. Ahlers, E. O. Goebel, S. Nau, T. Torunski, and W. Stolz, J. Appl. Phys. **94**, 2464 (2003).
[9] C. W. Tu, R. C. Miller, B. A. Wilson, P. M. Petroff, T. D. Harris, R. F. Kopf, S. K. Sputz, and M. G. Lamont, J. Cryst. Growth **81**, 159 (1987); S. Charbonneau, T. Steiner, M. L. W. Thewalt, E. S. Koteles, J. V. Chi, and B. Elman, Phys. Rev. B **38**, 3583 (1988).
[10] R. D. Dupuis, J. G. Neff, and C. J. Pinzone, J. Cryst. Growth **124**, 558 (1992).
[11] T. F. Kuech, E. Veuhoff, T. S. Kuan, V. Deline, and R. Potemski, J. Cryst. Growth **77**, 257 (1986).
[12] A. Rudra, E. Pelucchi, D. Y. Oberli, N. Moret, B. Dwir, and E. Kapon, J.

Cryst. Growth **272**, 615 (2004).
[13]Compare, for example, G. Bastard, C. Delalande, M. H. Meynadier, P. M. Frijlink, and M. Voos, Phys. Rev. B **29**, 7042 (1984); Jan P. van der Ziel, Xuefei Tang, and Ralph Johnson, Appl. Phys. Lett. **71**, 791 (1997).
[14]H. C. Chui, B. E. Hammons, N. E. Harff, J. A. Simmons, and M. E. Sherwin, Appl. Phys. Lett. **68**, 208 (1996).
[15]Toshiki Makimoto and Naoki Kobayashi, J. Phys. Soc. Jpn. **32**, L 648 (1993).
[16]R. K. Tsui, G. D. Kramer, J. A. Curless, and M. S. Peffley, Appl. Phys. Lett. **48**, 940 (1986); P. R. Hageman, J. te Nijenhuis, M. J. Anders, and L. J. Giling, J. Cryst. Growth **170**, 270 (1997); D. H. Zhang, C. Y. Li, and S. F. Yoon, *ibid.* **181**, 1 (1997).
[17]M. Shinohara, H. Yokoyama, and N. Inoue, J. Vac. Sci. Technol. B **13**, 1773 (1995).
[18]Special precautions were taken to avoid oxidation of the AlGaAs surface, by keeping these samples in a 6*N* nitrogen glove box before the AFM measurements. The samples were measured within a few hours from air exposure.
[19]We noticed a significant degradation in the photoluminescence and electrical transport quality if such precautions were not taken. The quartz "liner" which defines the reactor walls has to be periodically etched and cleaned to remove (Al)GaAs deposits. However, a growth with an uncovered susceptor results in sample surface temperature differences of a few tens of degrees between the uncovered and the covered case, given a same thermocouple reading. The impurity incorporation is also significantly higher in the uncovered case.
[20]The values on the x axis are the nominal ones (±0.02 degrees), with the exception of the cases where the step-flow pattern allowed unambiguously a direct estimation of the misorientation angle by AFM.
[21]These lowest values were not obtained all on the same sample.
[22]N. Moret *et al.* (unpublished).
[23]We stress that the undulations appearing in the flattened scans in Figs. 6 and 7 are artifacts of the flattening procedure. For example, the surface morphologies in Figs. 7(d) and 7(f) are indeed very similar, even if with a different spatial periodicity, ~0.5 μm and ~0.35 μm, respectively.
[24]M. Shinoara and N. Inoue, Appl. Phys. Lett. **66**, 1936 (1995), and references therein.
[25]A. Pimpinelli and A. Videcoq, Surf. Sci. **445**, L23 (2000); A. Videcoq, A. Pimpinelli, and M. Vladimirova, Appl. Surf. Sci. **177**, 213 (2001).
[26]G. Bernatz, S. Nau, R. Rettig, H. Jansch, and W. Stolz, J. Appl. Phys. **86**, 6752 (1999).
[27]A word of caution on this point is needed. The annealed cap morphologies do not necessarily reproduce the buried interface morphologies, as reported in Ref. 26 on "perfectly" oriented samples. On weakly misoriented substrates, however, we found that a strong correlation exists between the cap morphologies as measured by AFM and the buried interfaces morphology [N. Moret, D. Y. Oberli, E. Pelucchi, N. Gogneau, A. Rudra, and E. Kapon, Appl. Phys. Lett. **88**, 141917 (2006)].
[28]D. Kaufman, Y. Berk, B. Dwir, A. Rudra, A. Palevski, and E. Kapon, Phys. Rev. B **59**, R10433 (1999).